Thermochimica Acta, 145 (1989) 301–329
Elsevier Science Publishers B.V., Amsterdam – Printed in The Netherlands

NON-IDEALITY NEAR THE MONOTECTIC COMPOSITION OF A MISCIBILITY-GAP TYPE SYSTEM: SUCCINONITRILE–WATER

D.O. FRAZIER and B.R. FACEMIRE

Space Science Laboratory, NASA Marshall Space Flight Center, Huntsville, AL 35812 (U.S.A.)

(Received 20 October 1988)

ABSTRACT

Differential scanning calorimetry (DSC) of near monotectic succinonitrile–water solutions, fast-quenched in hydrophilic and hydrophobic DSC pans, indicate, by degree of undercooling, that there may be significant dependence of final ingot microstructure on the pre-quench equilibration temperature. Partial molal-volume determinations from density data, along with DSC data, suggest the nature of temperature dependent component associations from 20 °C to 55 °C in homogeneous solutions. The undercooling profile in a hydrophilic container is explained in terms of solution-composition shifts arising from the Gibbs surface excess. The evidence shows that temperature-dependent preferred component aggregates may modulate surface-composition gradients. Similar effects may be present through intermetallic compound formation in metallic monotectic alloys.

INTRODUCTION

Recent experimental work [1,2] shows that when a homogeneous binary solution is cooled toward the miscibility gap, critical adsorption of the phase having the highest chemical affinity for the container surface will occur. This observation agrees with the analysis of Fisher and DeGennes [3] who predicted that concentration near a wall is perturbed by the wall over a distance of the order of a correlation length. The result is that a layer of the preferentially wetting phase resides near the wall immediately above the critical temperature. Another very recent study made in this laboratory [4] demonstrates that a water-rich layer adjacent to a hydrophilic surface is present upon sectioning aqueous succinonitrile (SCN)-rich ingots fast-quenched through the miscibility gap. The object of this study was to explore the contribution that wall effects and component interactions make in solidification from a slightly hypomonotectic solution and to assess the phenomenon, as much as possible, in terms of the Gibbs surface excess. The Gibbs adsorption isotherm is

$$\Gamma = -\frac{a}{RT}\left[\frac{\mathrm{d}\gamma}{\mathrm{d}a}\right] \tag{1}$$

where Γ is the adsorption (excess concentration) of the solute at the surface, γ is the surface tension, a is the activity of the solute in bulk solution, R is the gas constant and T is temperature (K).

The central idea is that, classically, preferential adsorption of the component having the greatest affinity for the container will occur to some extent regardless of its proximity to the critical point. The nature of the adsorbed species should be directly dependent on the nature of intermolecular interactions occurring in the solution. Such surface effects may influence the apparent degree of undercooling in rapid-quenched samples by inducing concentration gradients. Surface : bulk-volume ratios will obviously be a significant determinant. The greater question of these studies, however, is the degree to which equilibrium conditions at the "soak" temperature influence ingot microstructure prior to a fast-quench. The effects here should be viewed primarily as a tool to infer differences in bulk ingot micromorphology as evidenced by differences observed after quenching in containers having different surfaces. The methods of analyses include differential scanning calorimetry (DSC) coupled with partial molal-volume determinations in homogeneous succinonitrile–water solutions.

Homogeneous miscibility-gap type solutions are, by definition, non-ideal near the coexistence curve, and hence must deviate from Raoult's law. Partial molal volumes are useful in indicating the nature of the association between the solution components. One aim of this work was to determine whether a hydrophilic surface in contact with a succinonitrile–water solution serves to reduce the bulk-solution free energy by providing an appropriate phase, in addition to the vapor space, to which water can escape. An aspect of this approach is to suggest the degree to which water adsorbed on a glass surface is associated with succinonitrile. It is therefore important to determine to what extent walls having opposite affinities for the aqueous minority phase affect the composition distributions. Furthermore, it is important to assess bulk-phase and surface composition variations, in homogeneous hypomonotectic solutions at temperatures above the monotectic temperature. Significant and persistent differences in solidification behavior in hydrophilic and hydrophobic cells, at different equilibration temperatures, could suggest the nature of preferred species in the homogeneous liquid phase. Finally, it is important to identify the fundamental effects that the equilibration temperature and surface affinities have on the solidified ingot phase distribution.

EXPERIMENTAL

Succinonitrile, purchased from Eastman Kodak Company, was purified by two vacuum distillations. Water, distilled and filtered to 16 mΩ cm resistivity was used to prepare the samples. A common stock solution of

TABLE 1

Density versus composition at selected temperatures

Temperature (°C)	Composition (wt.% H_2O)	Density (g ml^{-1})
13.5	91.73	1.00555
13.5	93.57	1.00469
13.5	100	0.99953
13.5	100	0.99934 [a]
21.5	8.25	1.01435
21.5	8.57	1.01415
21.5	91.73	1.00319
21.5	83.57	1.00214
21.5	100	0.99789
21.5	100	0.99791 [a]
23.5	8.25	1.01294
23.5	9.27	1.01279
23.5	9.65	1.0126
23.5	10.3	1.0122
23.5	91.73	1.00249
23.5	100	0.99745 [a]
25.9	8.57	1.0108
25.9	10.2	1.01053
25.9	91.73	1.00165
25.9	100	0.99663
25.9	100	0.99684 [a]
27.2	5.67	1.01012
27.2	6.56	1.0099
27.2	7.7	1.00967
27.2	8.57	1.00952
27.2	8.98	1.0095
27.2	10.34	1.00933
27.2	10.57	1.0093
27.2	11.4	1.00924
27.2	100	0.99649 [a]
31.2	5.56	1.00669
31.2	6.08	1.00653
31.2	6.64	1.00644
31.2	7.47	1.00624
31.2	8.09	1.00611
31.2	9.14	1.00599
31.2	9.98	1.00593
31.2	10.43	1.00584
31.2	10.86	1.00581
31.2	12.6	1.00567
31.2	100	0.99531 [a]
35.4	8.01	1.00296
35.4	13.95	1.00187

TABLE 1 (continued)

Temperature (°C)	Composition (wt.% H_2O)	Density (g ml^{-1})
35.4	93.57	0.99635
35.4	100	0.99347
35.4	100	0.99392 [a]
37.15	6.19	1.00123
37.15	6.97	1.0011
37.15	7.29	1.00103
37.15	8.08	1.0078
37.15	9.15	1.00058
37.15	10.38	1.00044
37.15	11.92	1.00029
37.15	13.13	1.00025
37.15	14.41	1.00015
37.15	100	0.99331 [a]
39.8	8.01	0.99903
39.8	8.2	0.99829
39.8	9.8	0.99803
39.8	9.8	0.99804
39.8	9.8	0.99805
39.8	12.43	0.99778
39.8	14.04	0.99768
39.8	15.54	0.99763
39.8	15.54	0.99761
39.8	16.15	0.99765
39.8	100	0.00232 [a]
41.2	11.18	0.9974
41.2	16.9	0.997
41.2	80.4	0.997
41.2	86.6	0.99618
41.2	89.04	0.99566
41.2	93.57	0.9936
41.2	100	0.99178 [a]
50.8	8.01	0.98937
50.8	10.91	0.98918
50.8	86.63	0.9907
50.8	93.57	0.989
50.8	100	0.98728
50.8	100	0.9877 [a]
60.8	5	0.98148
60.8	6.61	0.98078
60.8	8.39	0.98038
60.8	13.08	0.97954
60.8	15.43	0.97937
60.8	18.11	0.97922
60.8	25.61	0.97929
60.8	32.7	0.97977

TABLE 1 (continued)

Temperature (°C)	Composition (wt.% H_2O)	Density (g ml^{-1})
60.8	39.82	0.98029
60.8	42.78	0.98072
60.8	47.93	0.98109
60.8	50.17	0.98116
60.8	56.4	0.98158
60.8	60.59	0.98203
60.8	63.39	0.98229
60.8	73.04	0.98303
60.8	75.69	0.98321
60.8	77.62	0.98333
60.8	81.58	0.98347
60.8	83.71	0.9835
60.8	86.06	0.98349
60.8	89.2	0.98338
60.8	91.32	0.98331
60.8	100	0.98281 [a]

[a] Literature values.

8.7 ± 0.1 wt.% water was the sample source for all DSC runs. A Mettler DL18 Karl Fischer titrater measured sample compositions to ± 0.1 wt.% water. Perkin–Elmer stainless-steel large-volume capsules (75 μl, diameter 7.54, height 2.79 mm) were used as models to fashion the glass DSC cells used in this study. Two such cells were required for each sample withdrawn from the stock solution: one to remain hydrophilic; the other siliconized to be hydrophobic. The method of siliconizing the surface was identical to that outlined in a previous publication [4]. Prior to filling the cells with sample, Stycast 2850 FT epoxy was carefully applied to the outside bottom section of each cell. The hydrophobic cell bottom was first sanded to roughen the otherwise smooth siliconized surface prior to applying the epoxy. At this point, an aliquot of sample was withdrawn from the stock solution with a syringe and weighed by difference into each cell. (The same aliquot in the syringe was used for both cells to ensure that each contained identical samples.) The cells were immediately closed by firmly seating their lids and allowed to dry overnight. The total cell and content weights were recorded. Any cell weight loss was assumed to be due to leakage and invalidated its further use because of uncertainty of the solution composition. A Perkin–Elmer DSC 4 with Intracooler I and TADS data station was used to obtain the thermal data. Generally, the experimental approach was to equilibrate the homogeneous succinonitrile-rich solution in its sealed glass DSC cell at the desired temperature and then to quench it quickly to -50 °C while recording the heat profile. To assess the effect of the hydrophilic surface, the same process was repeated in the hydrophobic glass cell.

An important aspect of the method was to maintain the equilibration temperature for relatively long periods of time and to cool the cells quickly enough to minimize the readjustment of the composition distributions established at the equilibration temperature. Differences between the resultant thermograms should be partially indicative of the spatial composition gradients, at a given equilibration temperature, induced by wall effects. Vapor space effects seemed to be minimal, as discussed later.

A Mettler/Paar DMA 602 HT digital density meter was used to measure densities at several temperatures in homogeneous succinonitrile–water solutions (Table 1). Densities are required to determine the partial molal volumes of solute (water) to correlate with the thermograms from the DSC measurements. For the density measurement, the sample was placed into the remote measuring cell of the density meter. The natural vibrational frequency of a connected hollow oscillator was modulated depending on the density of the sample in the cell.

Differential scanning calorimetry

Figure 1(a) shows the typical thermogram obtained by quenching a succinonitrile–water solution containing 8.7 ± 0.1 wt.% water. In hydrophilic cells, the thermogram always contains three prominent exotherms. The assignments are as follows: (1) the large exotherm near 0 °C is the undercooled monotectic reaction (equilibrium temperature = 18.82 °C [6]—the calorimeter calculates heat on the basis of total sample); (2) the exotherm near −20 °C is assigned to the undercooled eutectic phase (equilibrium temperature = −1.36 °C [6]); (3) the exotherm near −44 °C is assigned to a solid–solid transition which triggers completion of eutectic-phase solidification [7]. A 5 °C min^{-1} scan of pure succinonitrile in a stainless-steel DSC pan showed a small exotherm onset at −43.52 °C of −0.08 cal g^{-1} (Fig. 2). This is equivalent to ca. 6.5 cal mol^{-1} and is believed to coincide with the solid–solid transition. There are three stable rotational conformers of succinonitrile (Fig. 3). It is generally agreed that the *gauche* conformers are 360 cal mol^{-1} more stable than the *trans* ones [8]. All the plastic crystal type substances used for modelling metallic solidification have low entropies of fusion at the normal freezing point and are characterized by a cubic crystal habit that transforms at a lower temperature. The very small exotherm at −43.5 °C indicates that when the succinonitrile solid is cooled to this temperature, about 98% conversion to the *gauche* conformers proceeds until a totally ordered phase is formed, which consists only of the *gauche* conformations. Both *trans* and *gauche* conformers coexist in solution, and in strongly dipolar solvents, the relative stability of *gauche* over *trans* is enhanced [9]. In SCN/H_2O the magnitude of the exotherm near −44 °C is about a factor of 25 times larger than the pure succinonitrile conversion; therefore, a second aspect of the peak in solution is assigned to

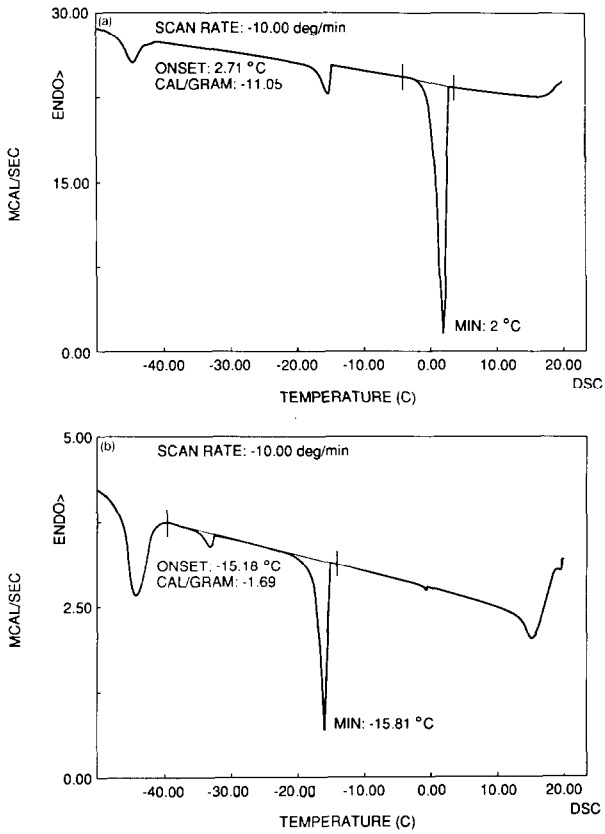

Fig. 1. (a) Typical thermogram after equilibration of succinonitrile–water solution in hydrophilic cells. (b) Example of a thermogram after equilibration of succinonitrile–water solution in a hydrophobic cell; the profiles tend to be random.

the solidification of the remaining water-rich phase which was isolated in the monotectic bulk at the instant of the monotectic reaction. Presumably, greater undercooling of this portion of the unsolidified water-rich phase is possible if very small and well-isolated pockets of eutectic clusters are not large enough to form the distribution necessary for the ice structure. Water has been known to undercool in emulsified form to about $-40\,^{\circ}C$ in the laboratory [10]. There may be a "triggering" of ice formation of the matrix isolated water-rich phase by the succinonitrile transformation.

The sum of the integrations of the two exotherms near $-20\,^{\circ}C$ and $-44\,^{\circ}C$ should approximate the heat of fusion of water if contributions to these exotherms were totally from water input. On the contrary, the respective sums are about half the value required to account for all the available water (3.60 cal g^{-1} vs. 6.80 cal g^{-1}). At relatively fast cooling rates, ($10–35\,^{\circ}C\ min^{-1}$) it is not possible to avoid exceeding the cooling capacity of the Perkin–Elmer Intracooler I with the DSC-4 at temperatures colder

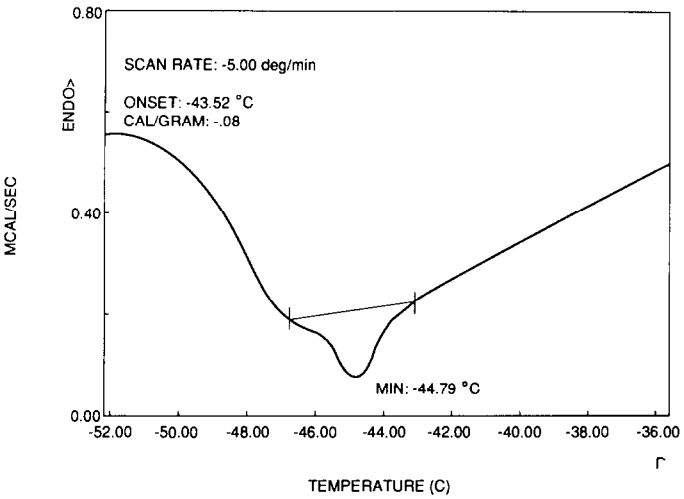

Fig. 2. Thermogram of pure succinonitrile cooled at 5 °C min^{-1} in a stainless-steel DSC pan. The exotherm at −43.52 °C is assigned to the final conversion of *trans* succinonitrile to the *gauche* rotamer.

than approximately −40 °C. Since it is not feasible to maintain good instrument control below −40 °C at high cooling rates, ice formation below this temperature cannot be measured quantitatively. A scan at slower cooling rates, 2 °C min^{-1}, though too slow for the resultant thermogram to be quantitatively representative of the initial high-temperature concentration distribution, allowed cooling to −55 °C while maintaining good temperature control. The sum of the two peak integrations increased to 4.4 cal g^{-1} [Fig. 4(a)]. Heating the sample from −55 °C to 60 °C at 10 °C min^{-1} produced two endotherms [Fig. 4(b)]: one was centered around 0 °C with a heat absorption of 4.2 cal g^{-1}; the onset of the other was at about 23 °C with a heat absorption of 12.23 cal g^{-1}. The occurrence of only two endotherms upon heating strongly suggests the combination of two of the

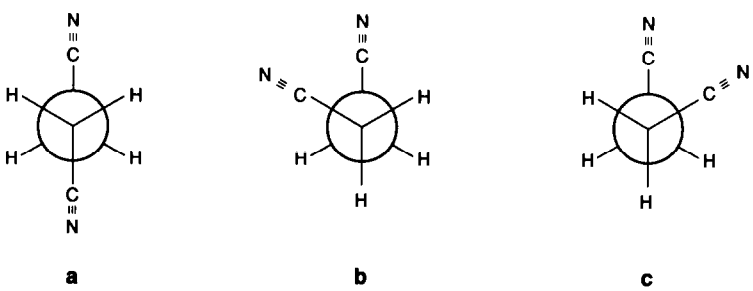

Fig. 3. *trans* and *gauche* rotamers of succinonitrile.

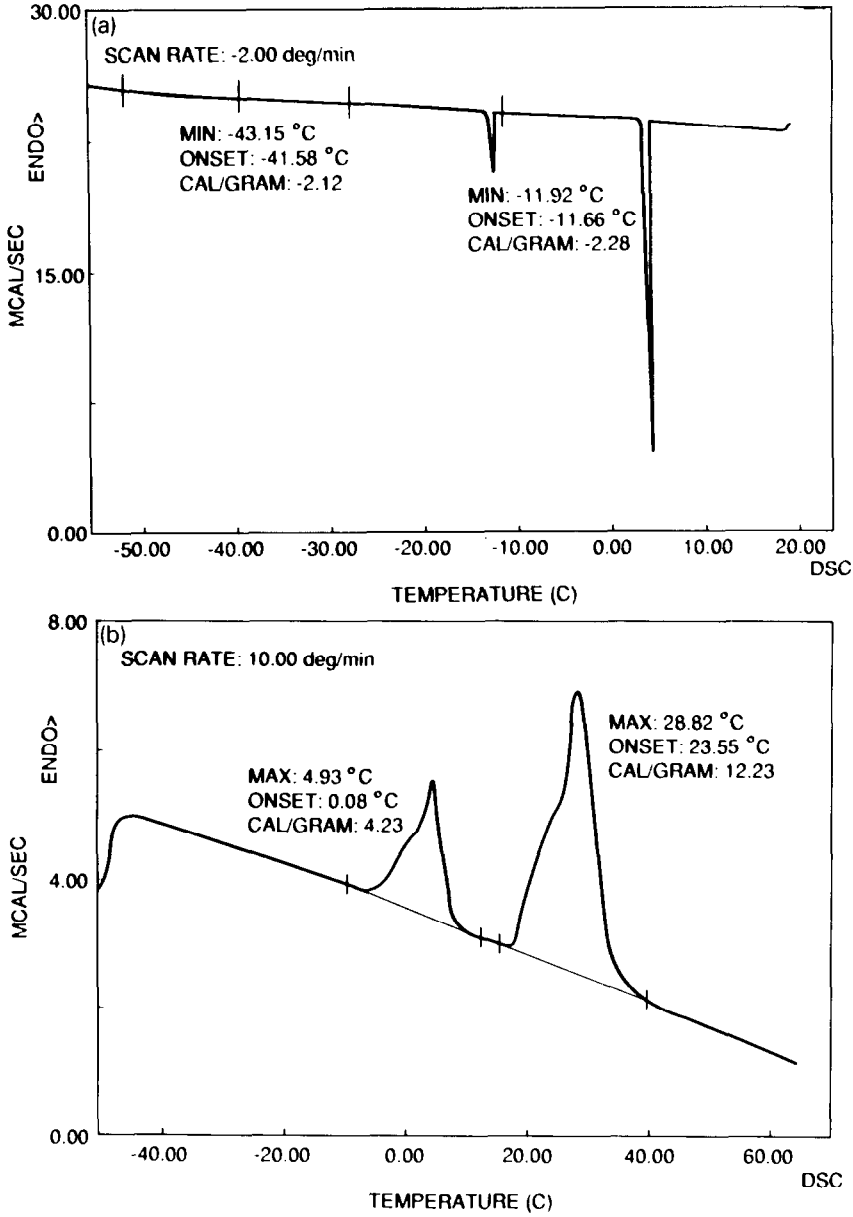

Fig. 4. (a) Sum of integration of two water-rich peak assignments. (b) Heating curves and assignments coinciding with cooling curves given in Fig. 3(a).

three cooling exotherms; furthermore, they joined at around 0 °C, the normal melting point of ice. The second endotherm in the heating curve appears around 23 °C, a temperature about 4 °C higher than the monotectic conversion. Since the heating curves tend to corroborate the assignment of the −20 °C and −44 °C exotherms as water-rich phases, it follows that the

unaccounted for water either never converted to ice (at least as low as $-55\,^{\circ}C$), or that the missing water, unlike the isolated pockets of the water-rich phase, forms a solid solution with succinonitrile at the monotectic conversion. There is no evidence of the presence of pure succinonitrile, since the melting endotherm returns to its baseline at about $40\,^{\circ}C$ indicating that succinonitrile and water are in fairly intimate contact throughout the monotectic solid.

Figure 1(b) is a thermogram profile obtained upon cooling in the hydrophobic cell a solution identical to that in the hydrophilic cell (both cells were filled from the same syringe at the same time). Figure 1(b) is directly comparable with the thermogram given in Fig. 1(a). In both cases, the cells and contents were held at $20\,^{\circ}C$ for 2 h prior to quenching at $10\,^{\circ}C\ min^{-1}$. In this particular run in the hydrophobic cell, there was no tendency for the monotectic reaction to undercool. In fact, the onset of the exotherm near $20\,^{\circ}C$ was above the monotectic temperature. The only way in which this can occur is if there is a composition shift, due to an absence of water, sufficient to move a local composition below the liquidus line where succinonitrile crystals can appear. We suggest that water depletion occurred at the hydrophobic surface during equilibration at $20\,^{\circ}C$ prior to quenching. Homogeneous solutions, at room temperature, transferred from hydrophilic to hydrophobic cells contained water-rich droplets primarily resulting from a surface excess in the hydrophilic cell. This is evidence that water is depleted at a hydrophobic surface. The other two primary exotherms appear near their usual locations with minor exotherms included in the profile. These patterns are reproducible in other hydrophilic versus hydrophobic runs. A scan at $5\,^{\circ}C\ min^{-1}$ to $-70\,^{\circ}C$ (thermal control off at $-47.5\,^{\circ}C$) to qualitatively observe any additional ice formation showed no new exotherms. The low temperature was maintained for about 2 h to allow any additional available water to freeze. The sample was reheated at $10\,^{\circ}C\ min^{-1}$ to $60\,^{\circ}C$. Again, the $0\,^{\circ}C$ endotherm was $4.83\ cal\ g^{-1}$ and the other $11.82\ cal\ g^{-1}$. Both values and curve shapes were nearly identical to the previous results. It is unlikely that the low heat value for the $0\,^{\circ}C$ endotherm was due to water loss because the weight of the sample cell was constant for 100 days after the final cure of the epoxy. Furthermore, if the $0\,^{\circ}C$ endotherm represented all of the water, assuming no succinonitrile loss (the vapor pressure of succinonitrile is extremely low in solution) the composition would have shifted from 8.7 wt.% to 5.8 wt.% water. This would place the sample composition significantly to the left of the monotectic composition and the observed degree of monotectic undercooling (-2 to $5\,^{\circ}C$ from $18.82\,^{\circ}C$, T_m) would be extremely difficult, if not impossible, particularly at the lowest $2\,^{\circ}C\ min^{-1}$ cooling rate. These considerations, therefore, suggest that a significant amount of water is associated with succinonitrile to form a solid solution, and that the association coincides with the monotectic conversion.

The equilibration times associated with the thermograms discussed thus far were about 2 h. To assess whether or not the "equilibration" times were sufficiently long to achieve true equilibrium concentration distributions, equilibration times of about 15 h preceeded several runs. Figure 5(a) is a typical thermogram in a hydrophilic cell resulting from a 35 °C min^{-1} cooling rate after a 15-h equilibration at 20 °C. The heat profile is basically the same as described for 2-h equilibration times; i.e. the monotectic reaction appears at about 0 °C, the untrapped eutectic phase at about −20 °C, and a very small and gradual exotherm in the vicinity of −40 °C. As is typical at all very high cooling rates in hydrophilic cells, the resolution is diminished, although the general heat profile remains unchanged. Figure 5(b) shows the heating curve integrations which again indicate an endotherm of 4.8 cal g^{-1} centered around 0 °C, and another from 23 °C to 40 °C of 11.92 cal g^{-1}. This is quite similar to the heating curve of Fig. 4 which resulted from a somewhat slower cooling rate (10 °C min^{-1}) and a considerably shorter equilibration time (2 h). Figure 5(c) results from a 15-h equilibration at 35 °C prior to cooling at 35 °C min^{-1} and is similar to the thermogram in Fig. 4(a). Figure 5(d) shows the thermogram resulting from a 15-h equilibration in the hydrophobic cell at 20 °C prior to quenching at 35 °C min^{-1} to −50 °C. In particular, note the absence of a sharp monotectic reaction near 0 °C which is always present in the hydrophilic cells. The −20 °C exotherm is now slightly greater in intensity than is usually observed in the hydrophilic cells. The heating curve [Fig. 5(e)] shows the typical endotherms, one centered around 0 °C with an intensity of 4.33 cal g^{-1} and another with an onset at about 24 °C of intensity 12.06 cal g^{-1} and tailing off to about 60 °C. This is generally similar to the other heating curves with two exceptions: (1) no shoulder appears on the water fusion endotherm (0 °C); and (2) the monotectic endotherm tails off to 60 °C instead of the usual 40 °C. These two features may be caused by the presence of purer water and succinonitrile in the separated ingot which is indicative of a relatively clean separation of components (except for SCN–water solid solution formation). The absence of the monotectic exotherm on cooling must be due to the separation of water and succinonitrile (and its solidification) during the equilibration time at 20 °C, perhaps the result of a "chromatographic" effect induced by the hydrophobic surface.

The calorimetric data in hydrophilic cells demonstrates that at low-temperature equilibration a larger amount of water is somewhat strongly associated with succinonitrile in the adsorbed layer. At higher temperatures a small amount of relatively unassociated water is present in the adsorbed layer. Figure 6(a) shows a plot of eutectic heat (containing adsorbed water) versus "trapped water heat" (that portion of the eutectic which is distributed in pockets throughout the solid matrix and is "triggered" to freeze by the solid succinonitrile transition). After high-temperature equilibration, there is generally more "trapped" water than at low-temperature equilibration as

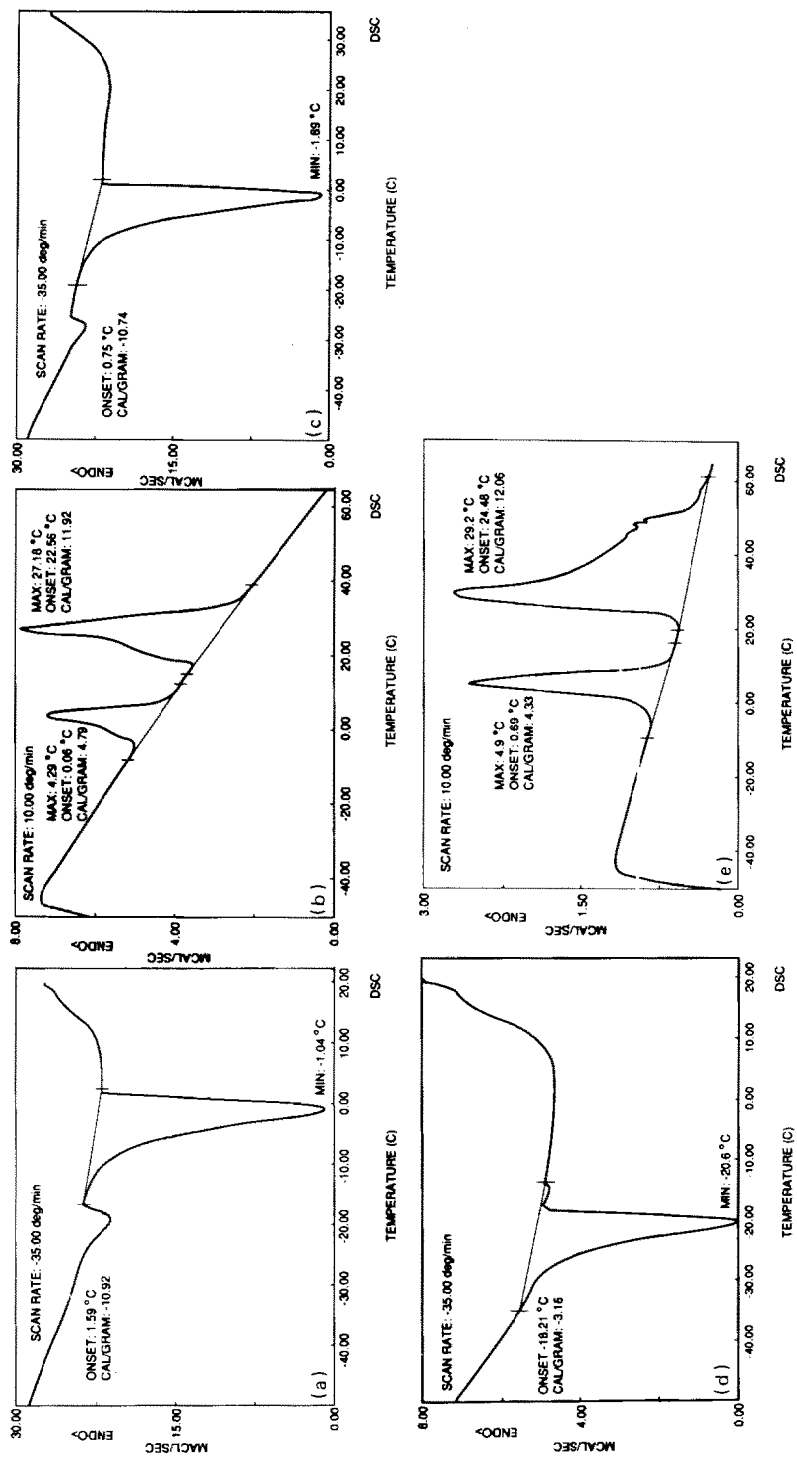

Fig. 5. (a) Thermogram (cooling rate 35 °C min^{-1}) of a succinonitrile–water solution which was equilibrated for 15 h at 20 °C in a hydrophilic cell. (b) Heating curve corresponding to the cooling curve in Fig. 4(a). (c) Thermogram (cooling rate 35 °C min^{-1}) of a succinonitrile–water solution which was equilibrated for 15 h at 35 °C in a hydrophilic cell. (d) Thermogram (cooling rate 35 °C min^{-1}) of a succinonitrile–water solution which was equilibrated for 15 h at 20 °C in a hydrophobic cell. (e) Heating curve corresponding to the cooling curve in Fig. 4(d).

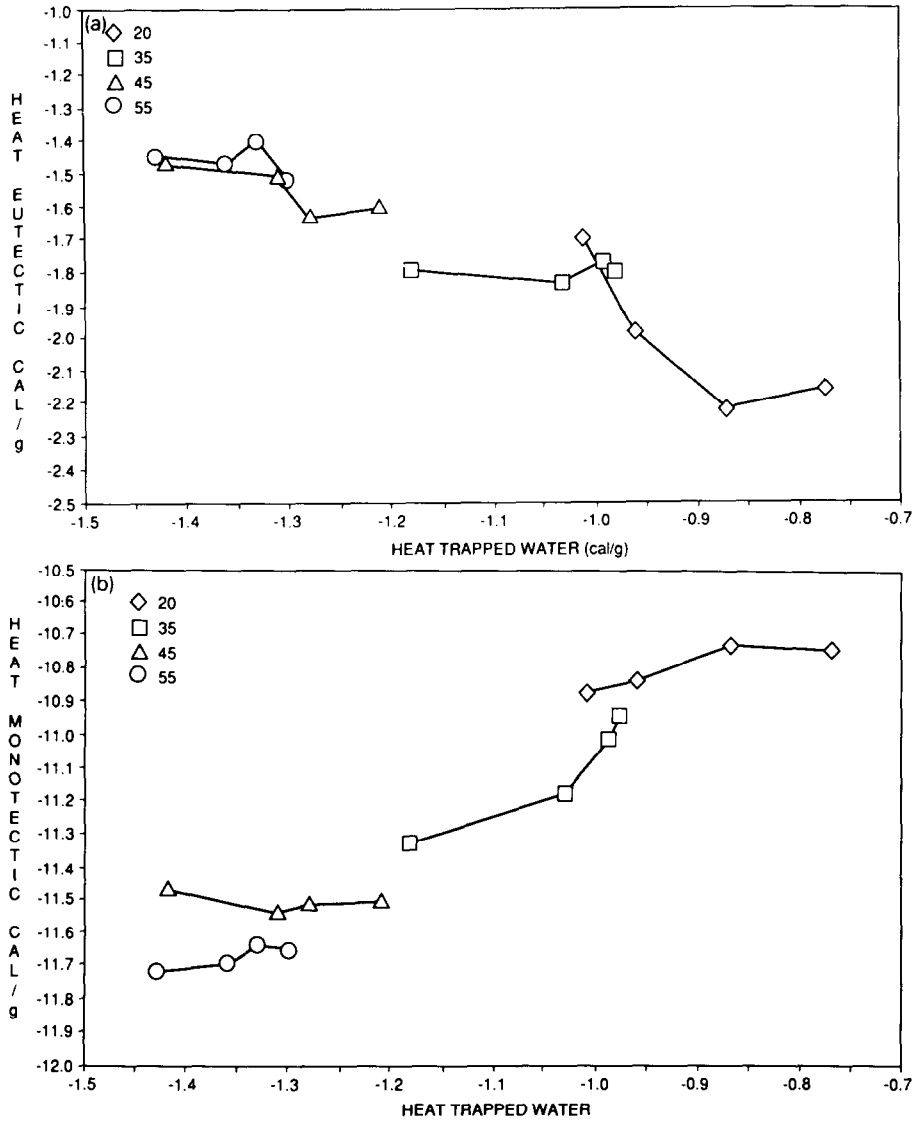

Fig. 6. (a) Eutectic heat (containing adsorbed water) versus trapped-water heat (portion of eutectic distributed in pockets throughout solid matrix). (b) Monotectic heat versus trapped-water heat.

determined by the associated heats of transition. Figure 6(b) demonstrates that the monotectic heat evolved is low at the low equilibration temperature suggesting that succinonitrile has been removed from the bulk by water capable of hydrogen bonding with the hydrophilic substrate. The low monotectic heat coincides with a small quantity of trapped water which, in accordance with Fig. 6(a) must correlate with a relatively large eutectic heat at $-20\,^{\circ}C$, hence a larger excess water adsorption at the hydrophilic

surface. The overall result of these occurrences is that equilibration at the highest temperature (55 °C) yields a Gibbs excess of H_2O at the hydrophilic surface with a sharper concentration gradient between the adsorbed layer and bulk. The excess exists also at the lowest equilibration temperature (20 °C), but with a much more diffuse gradient. A regular change in concentration of the adsorbed layer gives a situation between these two extreme equilibration temperatures.

STATISTICAL TREATMENT OF THE MONOTECTIC EXOTHERM

Figure 7(a) shows a plot of the monotectic solidification onset temperature versus the intensity of the monotectic exotherm for the 8.7 wt.% water solution quenched in a particular hydrophilic cell. Each data point was generated by the same solution sealed in a cell. The process of equilibrating and quenching was repeated in a different hydrophilic cell with a similar result. Two central aspects of this plot are: (1) because the absolute quantity of heat evolved (peak intensity) is an extensive property of the solidifying material, good correlation between onset temperature (extent of undercooling) and intensity is sufficient evidence that the extent of undercooling has some dependence on the quantity of the monotectic undergoing solidification; and (2) the smallest amount of undercooling occurs at the highest equilibration temperature (55 °C). The trend continues progressively down to equilibration at 20 °C which consistently provides the deepest undercooling. Of course, at the high quench rates, 35 and 10 °C min^{-1}, the time required to remove heat from the sample must be considered. If this were a dominant factor, the result would be that the hottest sample (55 °C) would appear to undercool the deepest; however, the opposite actually occurs. Figure 7(b) shows the same data for a hydrophobic cell filled simultaneously from the same syringe. The plotted data is quite different from that of Fig. 7(a). Since the amount of heat released is related to the amount of solidified material, it appears that the correlation in Fig. 7(a) may be due to a very slightly higher succinonitrile composition in the bulk phase at 55 °C than at 45 °C, and so on progressively down to 20 °C.

It is arguable that this effect is due to the presence of a vapor space in the cell which could accommodate increasing solution water fugacity as temperature increases. It was possible to approximate the vapor space volume by estimating the bubble diameter against the DSC-cell surface. The solution volume obtained by subtraction of the estimated bubble volume from the total cell volume, determined from the known internal cell dimensions, precisely matched the solution volume determined from the cell solution weight and density at room temperature. Assuming ideal solution and vapor behaviors, there is no appreciable solution composition shift due to water evaporation at any temperature used in this study.

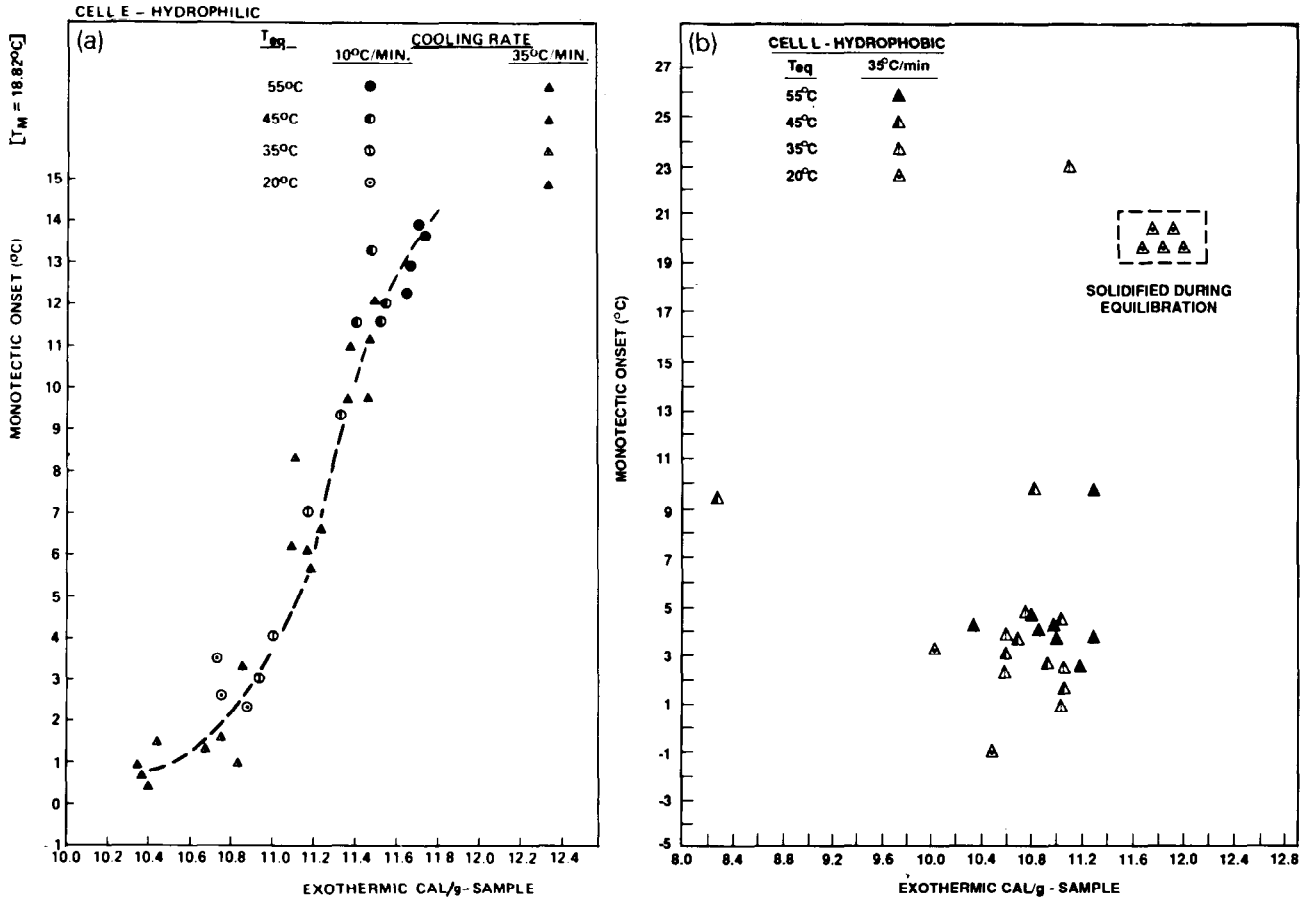

Fig. 7. (a) Monotectic solidification onset temperature versus the intensity of the monotectic exotherms from the thermograms developed during solidification in the hydrophilic cells. (b) Monotectic solidification onset temperature versus the intensity of the monotectic exotherm from the thermograms developed during solidification in the hydrophobic cells.

To support the hypothesis that wall effects are dominant, one must first support the quality of the correlation. It is somewhat reassuring to note that each 35 °C min^{-1} quench produces somewhat greater undercooling than its corresponding 10 °C min^{-1} quench equilibrated at the same temperature. However, in general, the greatest determinant of the extent of undercooling in the hydrophilic cell in fast-quenched samples is not the quench rate, although its effect is obvious, but, of this study's variables, the equilibration temperature.

The monotectic heat intensity is directly dependent on the quantity of succinonitrile undergoing solidification, hence the independent heat intensity variable is equated to succinonitrile concentration in the succinonitrile rich part of the solution undergoing conversion. The onset of monotectic solidification is not uniquely determined by the succinonitrile concentration (heat intensity). Other factors, such as quench rate, contribute to the monotectic onset temperature. It is possible to compare several independent data sets with respect to the variability about a regression line and to project some significance onto the pattern indicated in Fig. 7(a). Due to the difficulty in sealing hydrophobic cells, because the siliconized surface tends to reject adhesives, only one hydrophobic cell survived leak-free. Therefore, this cell, with its hydrophilic counterpart, was used as the basis for this analysis. These cells maintained constant weight throughout the test, which provides assurance that the sample compositions did not vary through leakage over the time-span of the experiment. The data sets may be grouped as follows (quench rate, equilibration temperature).

(1) Hydrophilic cell: (a) 35 °C min^{-1}, 20–55 °C; (b) 35 °C min^{-1}, 45 °C, 55 °C ($\leqslant$ 35 °C); (c) 35 °C min^{-1}, 20 °C, 35 °C ($\leqslant$ 35 °C); (d) 10 °C min^{-1}, 20–55 °C; (e) 10 °C min^{-1}, 45 °C, 55 °C ($>$ 35 °C); (f) 10 °C min^{-1}, 20 °C, 35 °C ($\leqslant$ 35 °C).

(2) Hydrophobic cell: (a–c) same as in (1).

Hydrophilic cell

"High" ($>$ 35 °C) and "low" ($\leqslant$ 35 °C) equilibration-temperature groupings can be used to compare the differences between fast-quenched and slower-quenched data as the equilibration temperatures increase from the monotectic temperature. By reducing the groupings from four (20, 35, 45, and 55 °C) to two ($>$ 35 °C and $\leqslant$ 35 °C), a greater number of data points become available per grouping. The results of several models, including a simple linear model, demonstrated that respective correlations of the variables were all comparable. Student's *t*-tests on linear models for group settings in (1) indicate that the monotectic onset and heat intensity are indeed dependent with 99.5% confidence of variability within one standard deviation in each grouping. There is, therefore, an appropriate statistical

relation between the monotectic onset and its intensity. Since good correlations were obtained from the simple linear models only these are discussed.

For groups (1b) and (1e), the correlation coefficients dropped from 0.928 to 0.604, respectively. The reduction in correlation may represent a tendency for the solution to lose its equilibration profile during slower quench rates, thereby allowing reordering as the solution senses cooler temperatures. For groups (1e) and (1f) the correlations were reasonably strong, 0.832 and 0.909, respectively. Considering all the equilibration temperatures together at a 35 °C min^{-1} quench rate (group 1a) the predicted values for the monotectic onset from the given values of heat intensity, had a slightly stronger correlation, $R = 0.923$, than at 10 °C min^{-1} (group 1d), $R = 0.915$. This could be the result of liquid-structure reordering during a relatively 'slow' quench. The corresponding R_s^2 suggest that 85.2% and 83.7%, respectively, of the variance between monotectic onset and heat intensity is due to the equilibration temperature with about 16% due to other factors. A χ^2 test on the data from the hydrophilic cell shows that the monotectic onset and heat intensity are dependent at a probability level of $p < 0.001$.

Hydrophobic cell

As indicated by Fig. 7(b), the monotectic onset versus intensity for solutions quenched in the hydrophobic cell appears nearly random. A linear model gave a negative correlation coefficient over the entire temperature range, 20–55 °C. A 10 °C min^{-1} quench was not part of the data. No possibility existed for a χ^2 test.

Partial molal volumes

With adequate support to establish a statistical relationship between monotectic onset and heat intensity from succinonitrile-rich SCN–water quenches in hydrophilic containers, it is useful to substitute the term "heat intensity" with "monotectic composition" to continue the discussion in terms of possible solution dynamics which may effect the nature of the short-range order in the homogeneous solution. Such order may be discussed in terms of partial molal volumes.

Non-ideality in miscibility-gap type solutions automatically opens the door to considerations regarding the relative intermolecular interactions between solution components. One of the most unambiguous measures of degree and direction of non-ideality are the experimental partial pressures of the solvent as compared to Raoult's law partial pressures. Another method of assessing the degree of component interactions is by comparing the partial molal volumes of the solute in solution with the molar volumes of the pure solute. The change in the partial molal volume of water with temperature was calculated as the hypomonotectic solutions approach the coexis-

tence curve. Evaluating partial molal volumes at 8.7 wt.% water (the composition of samples fast-quenched in the DSC cells) at a series of temperatures above the monotectic temperature allows correlation with the calorimetry data.

The partial molal volume of a solute is a measure of the volume change of a solution resulting from the addition of 1 mol of solute while holding the solvent volume constant. If successive 1-mol quantities of water are added to pure water at a constant temperature, T, and pressure, P, the volume will increase by the molar volume of water at T and P. When water is the solute in a binary mixture, as in the 8.7 wt.% water solution, the same volume change upon successive additions of 1-mol aliquots of water would indicate that the intermolecular forces were the same in the solution as in the pure component. Actually, however, the effective volume of the solute in solution may be quite different from its molar volume in the pure state. It is quite arguable that a significant change in the effective volume is due to the nature of the interactions between the solute and the solvent. The total volume change, an extensive solution property which adds a component to the solution while holding all other components constant at a given temperature and pressure, is the partial molal volume of the solution. It is convenient to use the molal volume because the solvent volume is, by definition, constant. The expression for the partial molal volume of solute in a binary solution is:

$$\bar{V}_A = \left(\frac{\partial V}{\partial n_A} \right)_{n_B, T, P} \tag{2}$$

where n_A is the number of moles of solute and n_B is the number of moles of solvent.

Assuming an infinite quantity of succinonitrile-rich solution to which 1 mol of water is added at a series of compositions at constant temperature imposes constancy of composition. Evaluation of $\bar{V}_A$ at some composition (primarily 8.7 wt.% water), is, therefore, unambiguous. Finally, the same measurement at various temperatures ascending from 20 °C and always including compositions of interest, provides a means of assessing the partial molal volumes at a series of temperatures at constant composition. For this reason, the method of determination used is an analytical application of the method of intercepts [11].

By the method of intercepts, we define a mean molar volume, V_m

$$V_m = \frac{V}{(n_A + n_B)} \tag{3}$$

where V is the volume of the solution and n_A and n_B are the total number of moles of the components; i.e. $V = V_m[n_A + n_B]$. Again, the partial molal volume, $\bar{V}_A$, is expressed by eqn. (2).

Hence, assuming constant temperature and pressure for the remaining equations:

$$\bar{V}_A = \left(\frac{\partial V}{\partial n_A}\right)_{n_B} = V_m + (n_A + n_B)\left(\frac{\partial V_m}{\partial n_A}\right)_{n_B} \tag{4}$$

Transforming $(\partial V_m/\partial n_A)_{n_B}$ into dV_m/dX_B, where X_B is the mole fraction of component B ($X_B = n_B/(n_A + n_B)$) gives

$$\left(\frac{\partial V_m}{\partial n_A}\right)_{n_B} = \frac{dV_m}{dX_B}\left(\frac{\partial X_B}{\partial n_A}\right)_{n_B} \tag{5}$$

therefore

$$\left(\frac{\partial X_B}{\partial n_A}\right)_{n_B} = \frac{-n_B}{(n_A + n_B)^2} \tag{6}$$

hence

$$\left(\frac{\partial V_m}{\partial n_A}\right)_{n_B} = \frac{dV_m}{dX_B}\left[\frac{-n_B}{(n_A + n_B)^2}\right] \tag{7}$$

Substituting expression (6) into eqn. (4) gives

$$\bar{V}_A = V_m + (n_A + n_B)\left(\frac{dV_m}{dX_B}\right)\left[\frac{-n_B}{(n_A + n_B)^2}\right]$$

and,

$$V_m = X_B\left(\frac{dV_m}{dX_B}\right) + \bar{V}_A \tag{8}$$

A plot of V_m versus X_B and a tangent to the curve at a definite mole fraction of component B will give the partial molal volume $\bar{V}_A$ at $X_B = 0$. The intercept at $X_B = 1$ is the partial molal volume of B, $\bar{V}_B$. To obtain the best form of an expression of mean molar volume in terms of mole fraction, statistical coefficients of linear and quadratic models of the data at each temperature were compared. A linear fit would impose a constant partial molal volume at all compositions approaching the miscibility gap. This would suggest that succinonitrile–water interactions were independent of composition. Clearly, this could not be the case in any system with a miscibility-gap. Quadratic models provide a better fit than linear models at all temperatures, supporting the hypothesis that solution interactions vary in a regular fashion with composition [Fig. 8(a)]. Molalities, determined by Karl Fisher titrations, and densitometry measurements of these solutions at various temperatures allow calculation of the mean molar volume. The appropriate quadratic expression of mean molar volume in terms of mole fraction was then determined. Partial molal volumes as functions of mole fraction were obtained for the solute and the solvent using the intercept

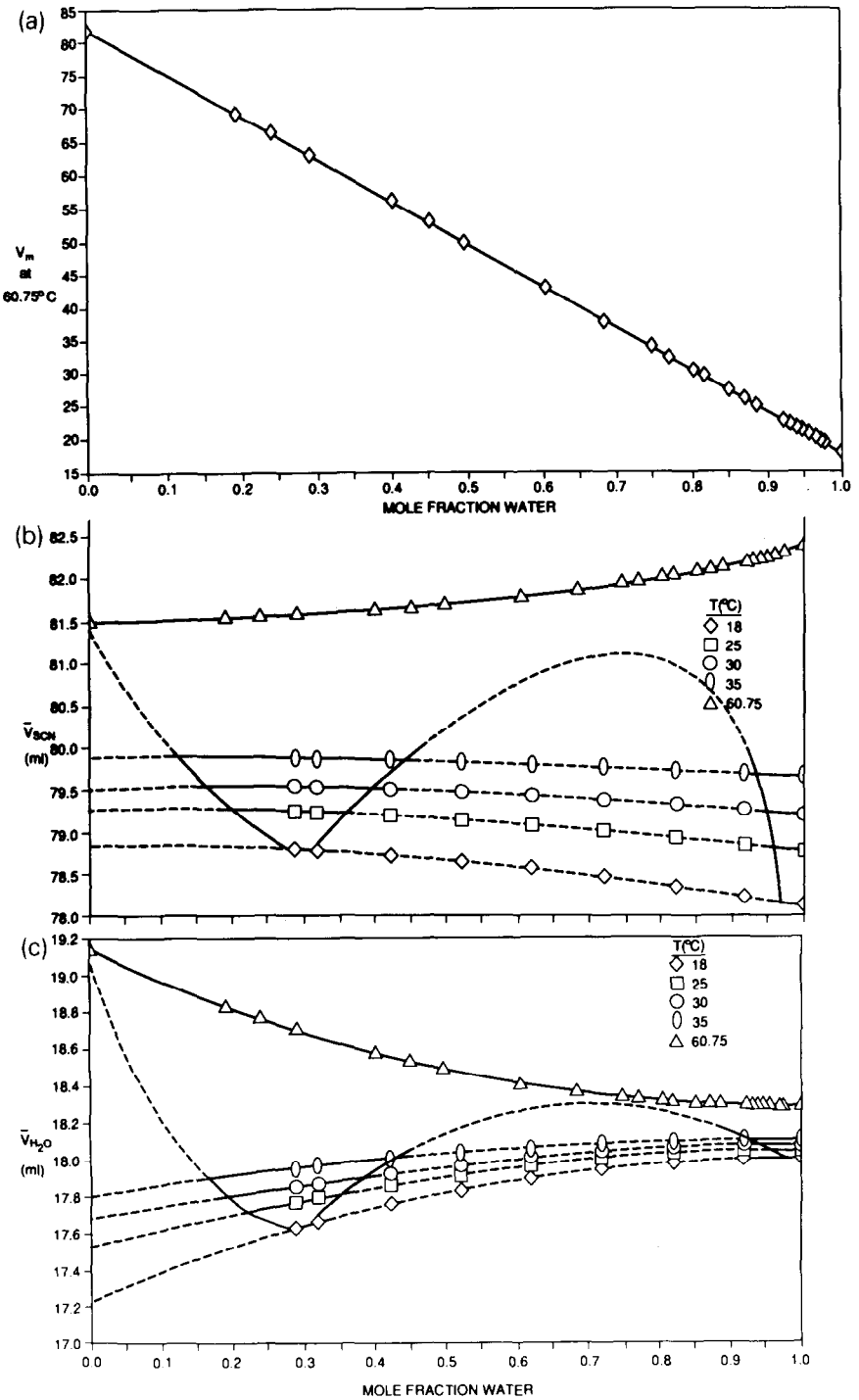

Fig. 8. (a) Mean molar volume versus the water mole fraction at 60.75 °C. (b) Isotherms of the partial molal volumes of water versus composition. (c) Isotherms of the partial molal volumes of succinonitrile versus composition.

TABLE 2

Partial molal volumes (PMV) of H_2O and succinonitrile in succinontrile–water solutions from density data

T (°C)	X_{H_2O}	PMV H_2O	PMV SCN
18	0.19	17.495	78.816
25	0.19	17.697	79.229
30	0.19	17.814	79.55
35	0.19	17.909	79.894
60.75	0.19	18.842	81.479
18	0.265	17.585	78.789
25	0.265	17.757	79.211
30	0.265	17.858	79.537
35	0.265	17.942	79.884
60.75	0.265	18.741	81.508
18	0.279	17.601	78.783
25	0.279	17.767	79.207
30	9.279	17.866	79.534
35	0.279	17.948	79.882
60.75	0.279	18.724	81.515
18	0.292	17.615	78.778
25	0.292	17.777	79.203
30	0.292	17.873	79.532
35	0.292	17.954	79.88
60.75	0.292	18.708	81.521
18	0.298	17.622	78.775
25	0.298	17.781	79.201
30	0.298	17.876	79.53
35	0.298	17.956	79.879
60.75	0.298	18.7	81.524
18	0.305	17.63	78.772
25	0.305	17.786	79.199
30	0.305	17.88	79.529
35	0.305	17.959	79.878
60.75	0.305	18.692	81.528
18	0.318	17.644	78.765
25	0.318	17.795	79.195
30	0.318	17.887	79.526
35	0.318	17.964	79.875
60.75	0.318	18.676	81.535
18	0.377	17.703	78.733
25	0.377	17.835	79.174
30	0.377	17.916	79.51
35	0.377	17.986	79.864
60.75	0.377	18.61	81.57
18	0.44	17.761	78.693
25	0.44	17.873	79.147
30	0.44	17.944	79.49
35	0.44	18.008	79.849
60.75	0.44	18.545	81.615
18	0.494	17.806	78.654

TABLE 2 (continued)

T (°C)	X_{H_2O}	PMV H_2O	PMV SCN
25	0.494	17.903	79.121
30	0.494	17.966	79.471
35	0.494	18.024	79.834
60.75	0.494	18.496	81.659
18	0.526	17.831	78.629
25	0.526	17.919	79.105
30	0.526	17.978	79.459
35	0.526	18.033	79.825
60.75	0.526	18.469	81.687
18	0.656	17.913	78.509
25	0.656	17.974	79.025
30	0.656	18.019	79.4
35	0.656	18.064	79.781
60.75	0.656	18.377	81.82
18	0.748	17.956	78.409
25	0.748	18.002	78.959
30	0.748	18.039	79.351
35	0.748	18.079	79.744
60.75	0.748	18.329	81.931
18	0.816	17.979	78.326
25	0.816	18.018	78.904
30	0.816	18.051	79.311
35	0.816	18.088	79.713
60.75	0.816	18.304	82.023
18	0.87	17.992	78.255
25	0.87	18.026	78.857
30	0.87	18.057	79.276
35	0.87	18.093	79.687
60.75	0.87	18.289	82.102
18	0.912	17.999	78.197
25	0.912	18.031	78.818
30	0.912	18.061	79.248
35	0.912	18.095	79.666
60.75	0.912	18.281	92.167
18	0.947	18.003	78.146
25	0.947	18.034	78.785
30	0.947	18.062	79.223
35	0.947	18.097	79.647
60.75	0.947	18.277	82.223
18	0.976	18.005	78.103
25	0.976	18.035	78.756
30	0.976	18.063	79.202
35	0.976	18.097	79.631
60.75	0.976	18.275	82.271
18	0.998	18.005	78.069
25	0.998	18.035	78.734
30	0.998	18.063	79.186
35	0.998	18.098	79.618
60.75	0.998	18.274	82.309

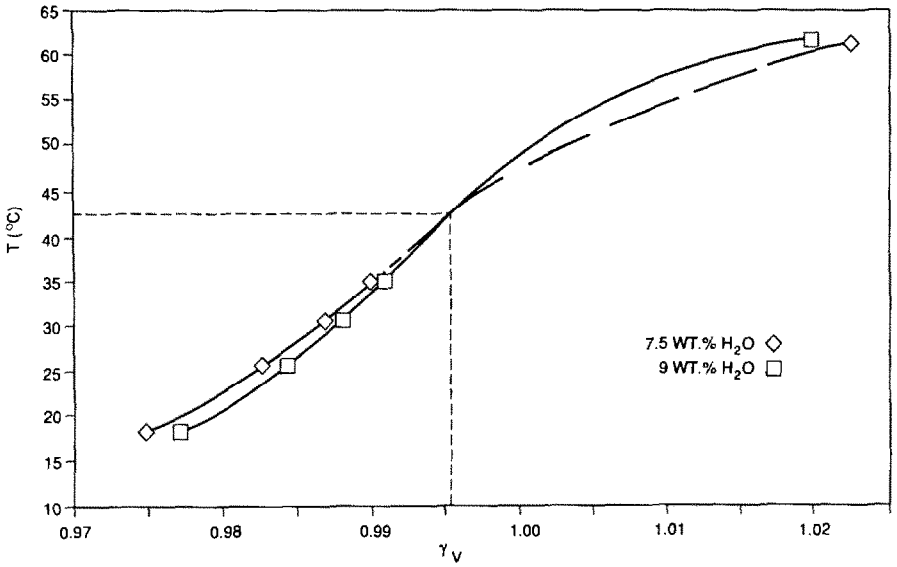

Fig. 9. γ_V versus temperature at two compositions.

method (Table 2). Figures 8(b) and 8(c) are plots of the partial molal volumes of succinonitrile and water, respectively, versus the mole fraction of water.

A measure of the deviation from solution ideality is defined by γ_V, the ratio of the partial molal volume of water in succinonitrile-rich solutions to the molar volume of pure water at a given temperature. Figure 9 shows a plot of γ_V versus temperature at two compositions. A curve ascends from a temperature near the miscibility gap. These isopleths are viewed as continuously increasing functions related to succinonitrile–water hydrogen bonding. At low temperatures, there are more hydrogen-bonded water and fewer succinonitrile molecules associated with "non-bonded" water from "mixture-model" theories [12–14], than at higher temperatures. Furthermore, at the higher temperatures, there may be more *trans* succinonitrile molecules in accordance with the relative temperature dependence of *trans/gauche* stability, and, therefore, even fewer water–water hydrogen bonds. Note that the two compositions in Fig. 9 have a common point near the isopycnic temperature, ca. 42 °C, and is near $\gamma_V = 1$, the condition at which a solution is traditionally considered ideal. Figure 9 is quite similar in shape to Fig. 7(a), the monotectic solidification onset temperature versus intensity. In the statistical treatment, we suggested that deviations from linearity in Fig. 7(a) may be due to loss of the equilibration temperature–composition profile at slower cooling rates. Conversely, the similarity in shape between Figs. 9 and 7(a) may suggest a correlation between equilibration temperature and solution-component interactions as a determinant to the degree of undercooling in samples having high surface/volume ratios and that linear correlations

for Fig. 7(a) are not strictly valid. It is generally accepted that undercooling affects the ingot micromorphology.

Suggested models

The quantity γ_V is less than unity at all concentrations approximately below the isopycnic temperature. The *trans* and *gauche* rotamers of succinonitrile have a relatively low barrier to interconversion (ca. 1.5 kcal mol^{-1}) with, as discussed, the *gauche* conformer dominating at lower temperatures [8,15]. A finite dipole moment for the *gauche* conformer and the zero dipole moment for the *trans* conformer must cause different succinonitrile–water interactions. As the temperature increases, the *trans*/*gauche* ratio also increases. We suggest the probability that water interacts both electrostatically and through hydrogen bonding with *gauche* succinonitrile, and that the *trans* conformer can only interact with water through hydrogen bonding. Low water accountability from the DSC data is mostly accountable if non-bonded (no H_2O hydrogen bonds) water, incapable of freezing, is a significant part of the monotectic reaction.

Figure 10 contains plots of water accountability versus the equilibration temperature at different cooling rates. Clearly, there is a consistent decrease in accountability as the cooling rates increase. However, water accountability is not significantly different between 10 °C min^{-1} and 2 °C min^{-1} indicating that low resolution due to rapid quenching is not a factor at 10 °C min^{-1} cooling. The maximum accountability is about 50% of the water in the sample. Furthermore, there is a slight decrease in accountability as equilibration temperature increases. The effect is most pronounced at the highest cooling rate, 35 °C min^{-1}. The result, at 10 °C min^{-1}, is that there is an approximately 5–7% accountability differential over the equilibration-temperature span of 20–55 °C. If we assume that the excess heat beyond the pure succinonitrile heat of fusion, observed in the monotectic reaction, is due to release of a small amount of lattice heat from succinonitrile bonded with non-bonded water (ca. 0.5 kcal mol^{-1}; hydrogen-bond strengths are typically 3–5 kcal mol^{-1} for NH bonds), then about 50% of the water is accountable as non-bonded water, incapable of freezing to an ice structure. Large quantities of non-bonded water excluded from a water mixture-model distribution because of associations with succinonitrile, is consistent with high partial molal volumes which are maximum at high temperature and low water content. At lower equilibration temperatures when the non-bonded water population tends to be lower, there are more water–water hydrogen-bonded structures and better accountability from the DSC freeze/melt data. A significant amount of water must remain relatively incapable of freezing over the entire temperature range, however, because accountabilities never exceed ca. 50%. This is true even at temperatures where the partial molal volumes are lowest. A fresh succinonitrile–water solution containing 9.32

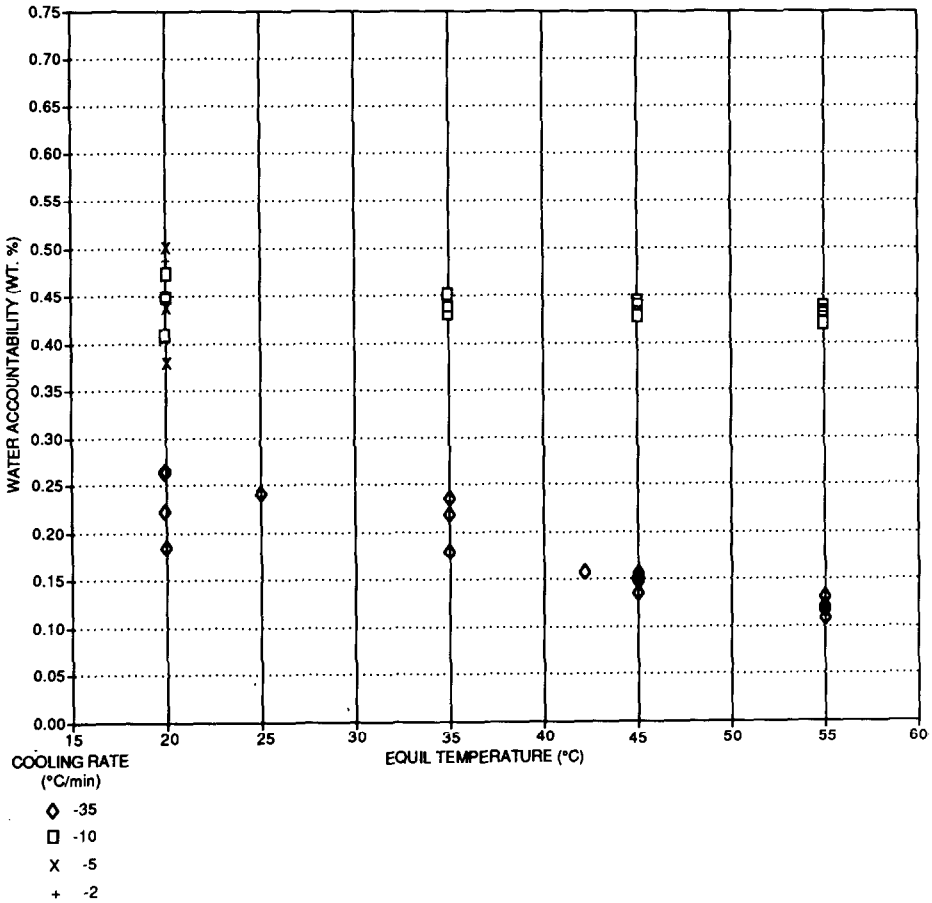

Fig. 10. Water accountability versus equilibration temperature at different cooling rates.

wt.% water was prepared, analyzed for precise water content and sealed in a conventional stainless-steel DSC pan. The water accountability increased to 70–75%. This still low accountability continues to support the presence of a strong water–succinonitrile interaction in the monotectic solid, but is 20–25% higher than accountabilities observed in the glass DSC pan experiments, which consistently gave values of 50% for both heating and cooling. There may have been some water loss during the relatively complex process of sealing the glass DSC pans. At 20% lower water content, however, the water concentration in the glass hydrophilic pan would be 7.1 wt.%, a water composition probably too low to achieve consistently high undercooling at 20 °C equilibration temperature, as observed in these experiments. Whereas the more efficient thermal conductivity of stainless steel as compared to glass can explain the discrepancies between the heating and the cooling data, it does not seem reasonable that a 20% composition error would give the

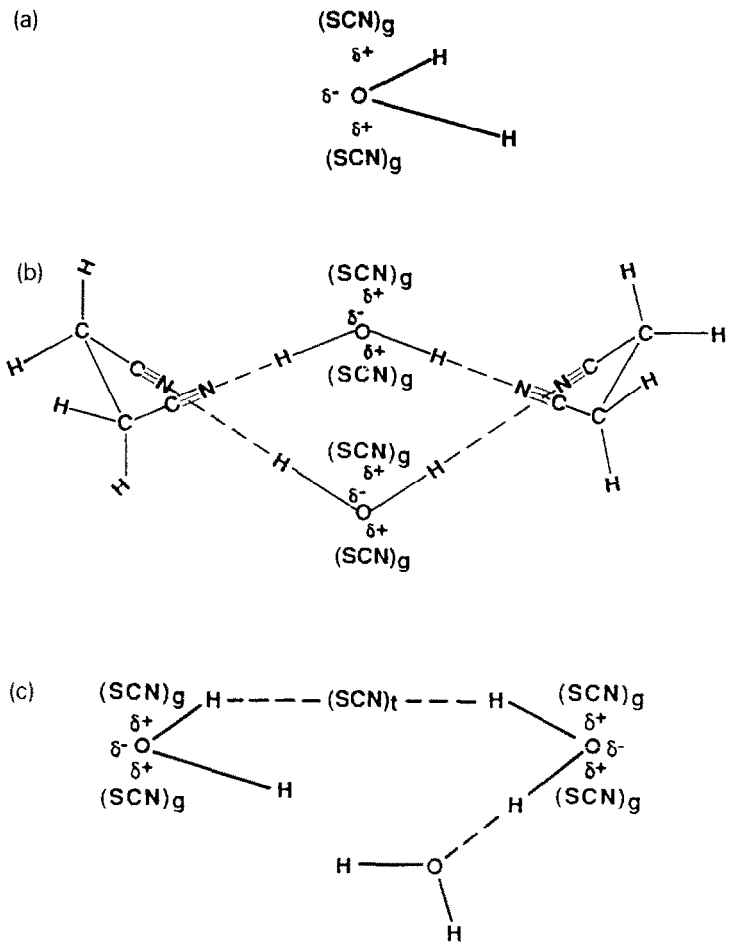

Fig. 11. (a) A model of *gauche* succinonitrile rotamers interacting electrostatically with water (10.11 wt.% H_2O). (b) A model of a six-membered ring structure (6.98 wt.% H_2O) involving *gauche* succinonitrile and zero-bonded water; this structure is unlikely to hydrogen bond to a hydrophilic substrate. (c) A model of an "open" structure capable of further hydrogen bonding and interaction with a hydrophilic substrate.

results which have been discussed above. Further analysis on this issue is required.

Figure 11(a) illustrates a suggested succinonitrile–water aggregate structure. The two succinonitriles surrounding oxygen are in *gauche* positions and interact electrostatically at their positive poles with the partially negative oxygen. This structure is 10.1 wt.% water and is near the monotectic composition (9.4 wt.%). The minimum water concentration observed in freshly solidified monotectic is 6.69 ± 0.46 wt.%. This was determined using monotectic solid which had not been allowed to warm above the monotectic temperature. This same composition may be achieved by bridging two

moities of Fig. 11(a) by hydrogen bonding with two *gauche* succinonitrile molecules. The resultant six-membered ring structure [Fig. 11(b)] has low ring strain and can interconvert between two chair conformations which coincide with the two succinonitrile *gauche* rotamers. This structure may be incapable of hydrogen bonding to a hydrophilic substrate. At high temperatures where the non-bonded water concentration is high, the latter would dominate. The eutectic water from the calorimetric data (ca. $-20\,^{\circ}C$ exotherm) of the hydrophilic cell contains less succinonitrile when equilibrating at $55\,^{\circ}C$ than at lower temperatures. "Interstitial" water-rich regions would be relatively succinonitrile free, and these clusters are likely to be attracted to a hydrophilic surface at equilibrium and be a major component of the adsorbed surface excess.

At lower temperatures, there are fewer non-bonded water molecules and, presumably, also less *trans* succinonitrile molecules available. Therefore, less succinonitrile participation via *trans* hydrogen-bonding, and more water–water hydrogen-bonded structures are likely. Figure 11(c) is an aggregate containing one SCN and one water hydrogen bonded to two moieties of Fig. 11(a). This structure is capable of hydrogen bonding to a hydrophilic substrate along with water-rich clusters. The presence of such an aggregate is consistent with observations in the calorimetric data that more succinonitrile is adsorbed onto the hydrophilic surface at low equilibration temperatures. This causes the bulk succinonitrile-rich solution to be succinonitrile "starved," with less monotectic reaction heat and deeper undercooling than following high-temperature equilibration. The decrease in the partial molal volume at 8.7 wt.% water, from $60\,^{\circ}C$ to $18\,^{\circ}C$, is about 6%. This is approximately the increase in water accountability from 55 to $20\,^{\circ}C$ in the calorimetric data, and may coincide with an effectively lower population of non-bonded water at $20\,^{\circ}C$ than at $55\,^{\circ}C$. Less non-bonded water causes more "open" hydrogen-bonded water type structures [Fig. 11(c)] than ringed structures [Fig. 11(b)]. Since the open structures are capable of water hydrogen bonding, they add to water accountability in the freeze/melt data.

DISCUSSION

The correlation between the DSC and the partial molal volume data suggests that the nature of the association between water and succinonitrile molecules varies with the equilibration temperature. Consequently, whereas at high temperatures a small amount of relatively unassociated water is present in the adsorbed layers in hydrophilic cells, a larger amount of more strongly associated water is in the adsorbed layer at lower temperatures. The former yields a fairly steep concentration gradient between the wall layer and bulk, whereas the latter results in a more diffuse gradient. Earlier observations of a thickening water-rich layer in fast-quenched suc-

cinonitrile–water solutions with increasing overall water concentrations may be better clarified by analyzing the nature of the proposed succinonitrile–water interactions as water concentration increases [4].

Indeed, the quadratic fits for the mean molar volume versus the mole fraction of water suggest that the intermolecular forces between SCN and water are dependent on the composition of the solution. Laser Raman and Fourier transform infrared (FTIR) spectroscopic studies [16,17] also indicate that the association of water and SCN are concentration dependent, and suggest that these differences are primarily due to differences in the hydration properties of the *trans* and *gauche* rotamers of SCN. The models shown in Fig. 11 help to explain the spectroscopically observed data.

Ab initio self-consistent field calculations on pure SCN with 4-31G** and 6-31G** basis sets [18–20] predict the *trans* rotamer to be the most stable, contrary to some of the experimental observations, with electronic energy differences of 1.24 and 1.25 kcal mol^{-1} by the respective basis sets [16]. Zero-point energy corrections and higher level calculations are in progress, however, and these may change these electronic energy differences. Also, at present, we are calculating the vibrational frequencies, thermodynamic parameters, etc., in order to ascertain the Gibb's free energy (ΔG) for the interconversion of the *gauche* and *trans* rotamers and to study the thermodynamics of hydration.

Optimization of the geometry of succinonitrile at the HF/6-31G level [18,20], and determination of the primary sites of hydration for the *trans* and *gauche* rotamers of SCN is in progress using the GAUSSIAN-86 program Version C. The MM2P software [21] is available through PROPHET for calculations on structures proposed in this paper. These results will also be compared with those of the ab initio calculations.

These considerations in an organic/water model system are, of course, not directly transferable to a metallic monotectic alloy. However, the effect of non-ideality in metals through intermetallic compound formation in homogeneous regions of miscibility-gap type solutions may deserve consideration by metallurgists. The very existence of a miscibility-gap may be a "signature" that solution-component associations are quite specific and, therefore, forbidden in the miscibility gap. Careful choice of the equilibrium temperature prior to a fast quench may require more knowledge of the solution than the mere location of the coexistence curve boundary.

ACKNOWLEDGEMENTS

The authors would like to thank Robbie Smith for his preparation of pyrex DSC cells, and Professor Jerry Shipman for helpful discussions. Also, we appreciate the work of Shelby Morris and Susan Burrer in preparing this manuscript.

REFERENCES

1 C. Franck and S.E. Schnatterly, Phys. Rev. Lett., 48 (1982) 763.
2 D. Beysens and S. Leibler, J. Phys. Lett., 43 (1982) L133.
3 M.E. Fisher and P.G. DeGennes, C.R. Acad. Sci., Sect. B, 287 (1978) 207.
4 D.O. Frazier, B.R. Facemire and U.S. Fanning, Acta Metall., 34 (1986) 63.
5 J.W. Cahn, J. Chem. Phys., 6 (1977) 3667.
6 J.E. Smith, Jr., D.O. Frazier and W.F. Kaukler, Scripta Metall., 18 (1984) 677.
7 C.A. Wulff and E.G. Westrum, J. Phys. Chem., 67 (1963) 2376.
8 B.H. Loo, Y.G. Lee and D.O. Frazier, J. Phys. Chem., 89 (1985) 4672.
9 J. Nowak, J. Malecki, J.M. Thiebaut and J.L. Rivail, J. Chem. Soc., Faraday Trans. 2, 76 (1980) 197.
10 M. Appleby, Clarkson University, private communication.
11 W.J. Moore, Basic Physical Chemistry, Prentice Hall, Englewood Cliffs, NJ, 1983, p. 178.
12 G.H. Haggis, J.B. Hasted and T.S. Buchanan, J. Chem. Phys., 20 (1952) 1452.
13 G. Nemethy and H.A. Scheraga, J. Chem. Phys., 66 (1962) 1773.
14 G.E. Walrafen, in A.K. Corington and P. Jones (Eds.), Hydrogen-Bonded Solvent Systems, Taylor and Francis, London, 1968.
15 K. Kveseth, Acta Chem. Scand., Ser. A, 32 (1978) 51. J.H. Hall and S.C. Bhatia, NASA-Annual Report, NAG8-088, 1988.
16 G.A. Walker, J.H. Hall and S.C. Bhatia, J. Phys. Chem., submitted.
17 B.H. Loo, D. Burns and D.O. Frazier, to be published.
18 H.F. Schaefer (Ed.), Methods of Electronic Structure Theory, Plenum Press, New York, 1977.
19 R. Ditchfield, W.J. Hehne and J.A. Pople, J. Chem. Phys., 54 (2) (1970) 724.
20 M.J. Frisch and J.A. Pople, J. Chem. Phys., 80 (7) (1984) 3265.
21 MM2P PROPHET Molecular Modeling System, NIH Sponsored Software Resource, 1985.